Review Article

Neuro MR: Protocols

David J. Mikulis, MD[1]* and Timothy P.L. Roberts, PhD[2]

Clinical MRI depends on a symbiosis between MR physics and clinical requirements. The imaging solutions are based on a balance between the "palette" of available image contrasts derived from nuclear spin physics and tissue biophysics, and clinical determinants such as the anticipated pathology and efficient use of imaging time. Imaging is therefore optimized to maximize diagnostic sensitivity and specificity through the development of protocols organized along the lines of major disease categories. In the other part of this two-part review, the primary determinants of image contrast, including T1, T2, and T2*, were highlighted. The development of pulse sequences designed to optimize each of these image contrasts was discussed and the impact of technological innovation (parallel imaging and high-field systems) on the manner in which these sequences could be modified to improve clinical efficacy was further emphasized. The scope of that discussion was broadened to include the application of: 1) water diffusion imaging used primarily for detection of pathologies that restrict the free movement of water in the tissues and for defining fiber tracts in the brain; 2) the intravenous administration of exogenous contrast agents (gadolinium-diethylene triamine pentaacetic acid [GdDTPA]) for assessment of blood-brain-barrier (BBB) defects and brain blood flow; and 3) MR spectroscopy (MRS) for assessment of brain metabolites. The goal of this part is to discuss how these acquisitions are combined into specific protocols that can effectively detect and characterize, or in keeping with our artistic analogy, "paint" each of the major diseases affecting the central nervous system (CNS). This work concludes with a discussion of image artifacts and pitfalls in image interpretation, which, in spite our best efforts to minimize or eliminate them, continue to occur. Much of the ensuing discussion is based on our own institutional experience. Protocols, therefore, do not necessarily match those from other institutions due to variability in clinical emphasis, MR instruments, and available software. An attempt was made to focus on basic clinical sequences that are available on most modern MR systems, with protocols employing generally accepted clinical imaging philosophies.

Key Words: MRI; imaging protocols; neuroimaging; pulse sequences; central nervous system
J. Magn. Reson. Imaging 2007;26:838–847.

THE TWO PRIMARY GOALS of clinical imaging are lesion detection and characterization. This is no different than any other clinical test in which sensitivity and specificity are of primary importance. The strategy is to optimize both, making the test as accurate as possible. In general, an easy way to improve accuracy is to image over longer periods of time, enabling an increase in signal-to-noise ratio (SNR) and spatial resolution. Patients, however, tend to move, especially when asked to remain in the MR system for extended periods of time (>30 minutes). Therefore, protocols are designed to be completed in 30- to 45-minute time slots that include a combination of actual scanning time, sequence setup time, patient positioning, and management time.

The next clinical issue of importance is visualization of brain lesions in more than one imaging plane. Multiplanar imaging enables more accurate definition of the relationship between lesions and normal adjacent structures. Since isotropic imaging has not yet proven time efficient, protocols should include pulse sequences that provide at least two orthogonal imaging planes for review.

Finally, since most lesions in the central nervous system (CNS) have increased water content and therefore demonstrate longer T1 and T2 relaxation times compared to normal tissue, T1-weighted and T2-weighted spin-echo pulse sequences are usually included in all brain protocols. From this point, the disease category dictates adjustments to these generalizations and governs the need for additional sequences, in which T2* contrast, diffusion, perfusion, blood-brain-barrier (BBB) breakdown, and metabolite information is essential.

The next section outlines protocols for the major categories of disease affecting the CNS, emphasizing the rationale behind the different "paints" used to characterize the abnormalities (Fig. 1). Please note that when specific sequence parameters are listed, they refer to 1.5T imaging.

[1]Department of Medical Imaging, The University Health Network, The Toronto Western Hospital, Toronto, ON, Canada.
[1]Department of Radiology, Children's Hospital of Philadelphia, University of Pennsylvania School of Medicine, Philadelphia, Pennsylvania, USA.
*Address reprint requests to: D.J.M., Associate Professor and Director of fMRI Research, Dept. of Medical Imaging, The University Health Network, The Toronto Western Hospital, Room 3MC-431, 399 Bathurst St., Toronto, ON M5T 2S8. E-mail: mikulis@uhnres.utoronto.ca
Received June 21, 2006; Accepted May 3, 2007.
DOI 10.1002/jmri.21041
Published online in Wiley InterScience (www.interscience.wiley.com).

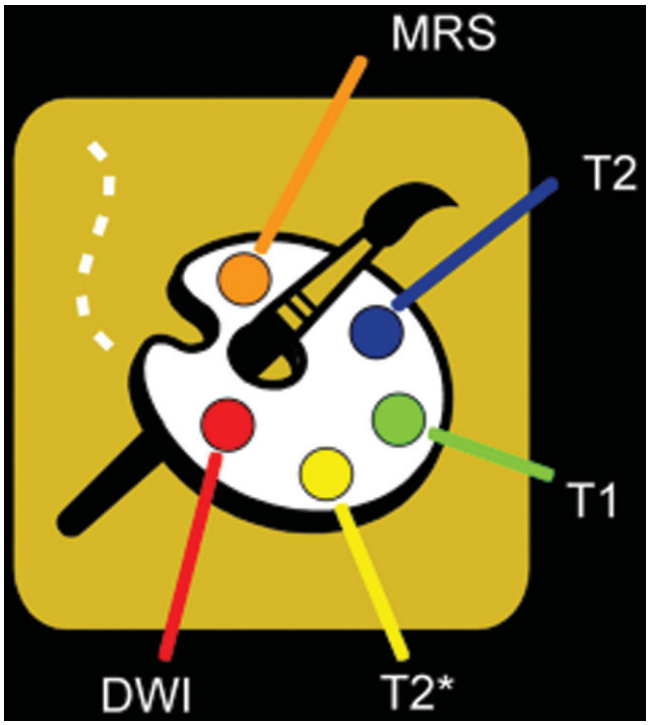

Figure 1. Image palette displaying the "paints" used for developing disease specific protocols.

SCREENING BRAIN PROTOCOL

The screening brain protocol is applied when patients present with nonspecific symptoms and typically have no localizing neurological signs, e.g., headache or deteriorating cognitive function. Basic multiplanar imaging selecting T1 and T2 "paints" from the imaging palette can effectively screen for the majority of brain lesions and can be achieved with just three pulse sequences: 1) sagittal T1 spin-echo; 2) axial T2 spin-echo; and 3) axial fluid attenuated inversion recovery (FLAIR) sequences. The FLAIR sequence, which nulls CSF (looks black), replaces the previous proton density (PD) standard for detecting long T2 lesions, especially those situated at CSF–brain interfaces (difficult to see a T2 bright lesion adjacent to bright CSF). FLAIR has also been deemed superior to T2 and PD for detecting lesions with increased T2 relaxation (1–3). We have chosen to add two additional sequences, not only to this basic screening protocol, but to all of our brain imaging protocols: T2* and diffusion (note: these sequences are not always mentioned separately in each of the protocols discussed). The T2* acquisition is a gradient echo sequence with TE = 30 msec, and an EPI diffusion sequence. The T2* sequence has a long TE, making it sensitive to the presence of iron in the brain parenchyma; it is very useful for assessing old and new hemorrhages. The diffusion sequence is added primarily to provide sensitivity to acute/subacute ischemia and requires only 35 seconds for full brain coverage. The time costs are minimal for the valuable information gained. Figure 2 shows each of the acquisitions in a 29-year-old patient presenting with headache, nausea, and vomiting, showing no abnormality on these sequences. The last image, labeled T1-Gd, is a gadolinium (Gd)-enhanced T1 sequence added only if there is a clinical indication, as described below.

SCREENING BRAIN WITH CONTRAST

If there is a clinical suspicion that the pathological process affecting the brain can disrupt the integrity of the BBB, then intravenous Gd is administered followed by T1-weighted spin-echo imaging. Common disorders associated with breakdown of the BBB resulting in extravasation of Gd and shortening of T1 include inflammation (multiple sclerosis), tumors, and infections. Figure 2 shows that all of the images are normal except for the Gd-enhanced T1 image. Without it, the extensive enhancement of the brain surface (leptomeninges) would have been missed. A diagnosis of herpes simplex meningitis was later established.

MULTIPLE SCLEROSIS (MS) PROTOCOL

MS is an autoimmune inflammatory condition directed against the myelin sheath of CNS axons. These lesions follow the principle of increased water content showing prolonged T1 and T2 relaxation, with the vast majority localizing as expected in the hemispheric white matter. Acute/subacute lesions are associated with BBB breakdown. Many lesions are seen in the periventricular white matter and can therefore be difficult to separate from CSF. It is therefore useful to apply either PD or CSF nulling sequences to distinguish these lesions from CSF spaces. For lesion visibility and detection, it is clear that FLAIR is superior to PD in the supratentorial white matter, but the opposite is true for posterior fossa lesions, where PD holds a significant advantage (note: on PD images, gray matter, white matter, and CSF all have relatively similar signal, whereas lesions such as MS plaques have higher signal. Similarly, lesions seen on FLAIR images are brighter than CSF and normal brain) (4). The reason for this is not entirely clear, al-

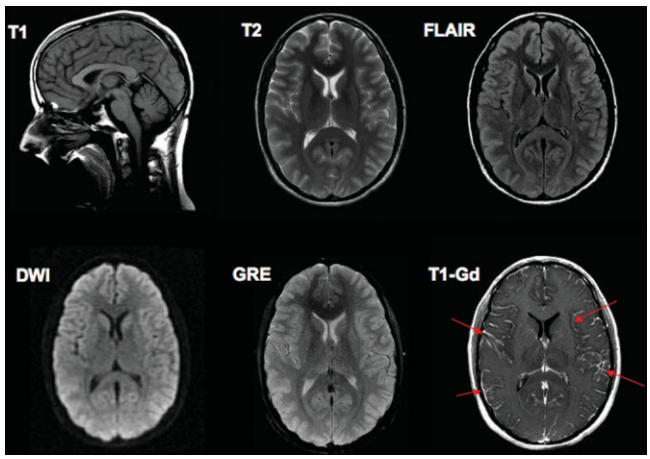

Figure 2. Screening brain protocol. This protocol employs T1, T2, T2*, and water diffusion parameters. Only the T1-Gd image is abnormal showing excessive nonvascular high signal caused by Gd leaking into the inflamed meninges (arrows) in a patient with herpes simplex meningitis.

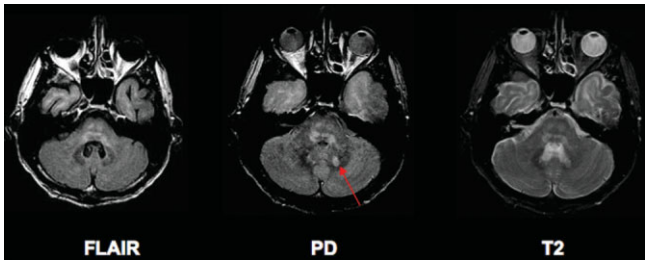

Figure 3. MS protocol. The PD sequence shows a plaque (arrow) in the dentate nucleus of a patient with multiple sclerosis, which could easily have been missed on FLAIR and T2.

though it has been suggested that the relatively long echo time used in FLAIR might be responsible for loss of contrast in lesions where T2 is not greatly elevated (4). The palette of contrasts required for this protocol are therefore modest, necessitating only T1 and T2 acquisitions. Figure 3 demonstrates the efficacy of the PD acquisition over FLAIR for detection of a posterior fossa MS plaque, as this lesion, which is difficult to separate from CSF on T2 since it merges with the bright CSF in the fourth ventricle, stands out on the PD image. The role of Gd-enhanced imaging in the diagnosis and management of patients with MS remains controversial. But a recent consensus statement advocates its use:—"Enhanced MRI is recommended for suspected MS for purposes of diagnosis and initial diagnostic evaluation." (5).

TUMOR PROTOCOL

The goal of using MRI as a surrogate for tumor histopathology, which originated with quantitative relaxation measurements, has never been realized. This has not, however, dampened efforts to improve tumor characterization (tumor type and tumor grade) through application of the full range of available morphological and functional tools. As always, the first step is to acquire T1- and T2-weighted images to establish the location and extent of the neoplasm. It is important to ascertain whether the tumor is arising from the brain substance itself (intraaxial), or from the meninges (extraaxial) since primary brain tumors as a family tend to be malignant. This can be difficult if only one imaging plane is obtained. Current protocols typically include multiplanar acquisitions to improve the accuracy of this determination. Assessment of the BBB through Gd administration is useful for grading primary tumors. Contrast enhancement indicates the presence of BBB leaks correlating with vascular proliferation and degree of malignancy; however, this correlation is not reliable. In a recent series of 21 glioblastomas, four showed no or minimal enhancement (6). Since these conventional approaches have failed to provide the desired diagnostic specificity, an array of functional/physiological approaches have been applied, using all of the remaining "paints on the palette" including T2*, diffusion, and MR spectroscopy (MRS). These can provide information on perfusion, vascular permeability, hydrogen metabolites, and neuronal fiber networks (Fig. 4). Each has shown varying degrees of correlation with tumor grade. Increases in cerebral blood volume (CBV) derived from perfusion data, increases in vascular permeability derived from dynamic bolus T1 measurements, decreases in apparent diffusion coefficients (ADCs), and increases in choline metabolites derived from MRS data have all been correlated with increasing tumor grade (7–11). No single method has shown accuracy, however, for determining tumor behavior or tumor type, e.g., discriminating astrocytoma from mixed oligoastrocytoma from oligodendroglioma. Building spatial multiparametric correlations from these variables in an attempt to identify tumor "hot spots" predictive of aggressive behavior prior to observable changes on conventional images is the focus of current research (Fig. 5). If successful, functional imaging could play a significant role in tumor surveillance and therapeutic monitoring. From a treatment planning perspective, the ability to identify the relationship between tumor tissue and nearby eloquent gray matter (e.g., language and motor cortex) and important white matter fiber tracts (corticospinal tract) is made possible through functional MRI (fMRI) and diffusion tensor tractography (DTI), which take advantage of T2* and directional water diffusion properties of the tissues (Fig. 6). These methods promise to improve the safety and efficacy of tumor resection through modifications in surgical planning and approach but outcomes research is currently lacking (12–14). The clinical challenge is to create a protocol that can maximize diagnostic sensitivity and specificity, provide prognostic information, and assist in treatment planning in a time-efficient manner. The major tradeoffs are time efficiency and image data postprocessing requirements.

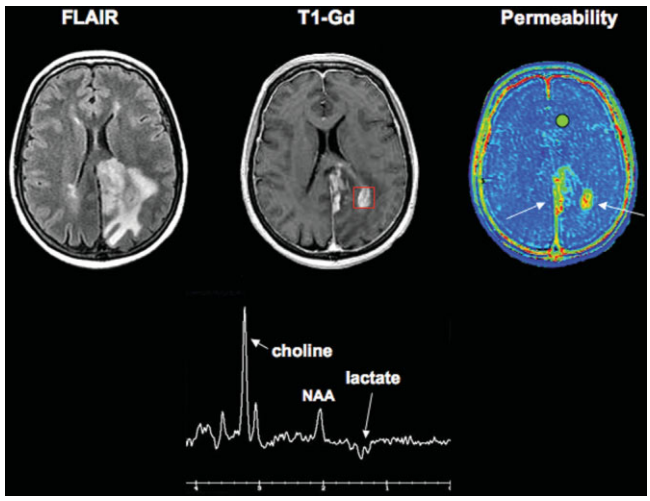

Figure 4. Physiological tumor imaging. FLAIR image shows a left occipital glioma containing focal areas of Gd enhancement on the T1-Gd image, one of which is outlined in a red box from which MRS data (shown below) were obtained. The choline peak is sharply elevated, indicating membrane proliferation; NAA, a marker of healthy neurons, is decreased; and lactic acid is present, indicating metabolic stress frequently associated with high-grade gliomas. The permeability image provides quantitative information concerning the rate of Gd leakage out of the tumor vessels. In this case, there is a central zone of high permeability (red) a feature that the conventional post-Gd T1 image does not show.

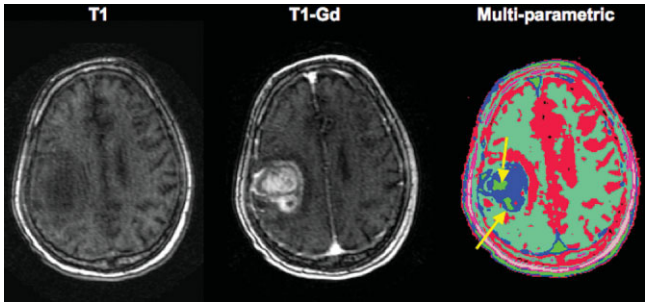

Figure 5. "Mixing the paints." T1 and T1-Gd images show an enhancing glioma. Correlational analysis using information from such parameters as T1, T2, DWI, blood volume, perfusion, permeability, and MRS data may eventually reveal distinctive regions within tumors that predict behavior. The multiparametric image on the right is an image derived from a statistical cluster analysis revealing areas within the tumor (yellow arrows pointing out green regions), where the cluster of parameters is significantly different from the rest of the tumor. Future work is needed to determine the clinical implications of these findings.

Current state-of-the-art MRI systems are capable of providing considerable anatomic and functional information about brain tumors; however, scan times can be lengthy even with parallel imaging–enabled systems. The design of a tumor protocol should ultimately be based on proof of impact on reducing morbidity and mortality and increasing the cost effectiveness of care. This type of information is currently limited (case reports or small series) or completely lacking. For example, can DTI be used to reduce the morbidity of surgery by identifying the relationship between tumor tissue and important white matter tracts? Each institution must therefore decide on protocol design based on the perceived importance of physiological information and the available resources, including patient volumes, scanner time, postprocessing expertise, etc. A state-of-the-art protocol would build on the foundation of the previously described screening brain protocol that includes post-Gd T1 images. The following functional/physiological sequences could then be added: 2D MRS, DTI, fMRI, permeability imaging, and dynamic-susceptibility contrast-enhanced MRI (DSCE-MRI) for measuring tumor blood volume. As more information concerning the relative clinical value of each of the physiological parameters becomes available, it may be possible to eliminate certain acquisitions to optimize efficiency.

EPILEPSY PROTOCOL

Epilepsy imaging, in addition to general screening of the brain for lesions with a propensity to cause seizures (primary brain tumors and vascular malformations), requires detailed assessment of cortical structures for neuronal migrational anomalies and low-grade cortical neoplasms (e.g., dysembryoplastic neuroepithelial tumor). Sequences focusing on the hippocampus and mesial temporal lobes must be applied in those patients with a history of partial complex seizures (Fig. 7). Fast 3D T1-weighted gradient echo acquisitions provide high spatial resolution with good gray/white discrimination for assessment of gray matter. Coronal (perpendicular to the axis of the hippocampus) short TI (to null lipid) inversion-recovery (IR) sequences with long TE render the hippocampus and mesial temporal lobes in exceptional detail, enabling the diagnosis of mesial temporal sclerosis. Occasionally, conventional MRI in patients with temporal lobe epilepsy is unrevealing. Additional imaging techniques have been applied in this setting in an attempt to isolate the abnormal hippocampus, including volumetric imaging of the hippocampal formations, high-resolution imaging of hippocampal anatomy at high field (3T), MRS, and DTI (Fig. 8). Reduction in hippocampal volumes correlate with electroencephalograph (EEG) findings but require edge detection algorithms and are not in routine clinical use due to lengthy times required for analysis (15). MRS can aid in identifying the abnormal hippocampus if reductions in N-acetyl aspartic acid (NAA), a marker of healthy neurons, is present (16,17). fMRI techniques have been applied to assess working memory as an adjunct to Wada testing (selective intraarterial injection of an anesthetic) to determine the functional status of the hippocampus prior to temporal lobe resection for medically intractable epilepsy (Fig. 7).

CEREBROVASCULAR IMAGING PROTOCOL

The two most important methods for imaging blood vessels depend either on T1 relaxation or flow-induced changes in spin phase. The latter, called phase contrast MR angiography (MRA), is not commonly used clinically and will not be discussed further. Two methods using T1 relaxation effects are available, i.e., non-contrast- and contrast-enhanced methods. The non-contrast-enhanced method depends on the inflow of unsaturated blood protons entering the imaging slice where the longitudinal magnetization of stationary protons is saturated via short TR. This results in high signal contrast

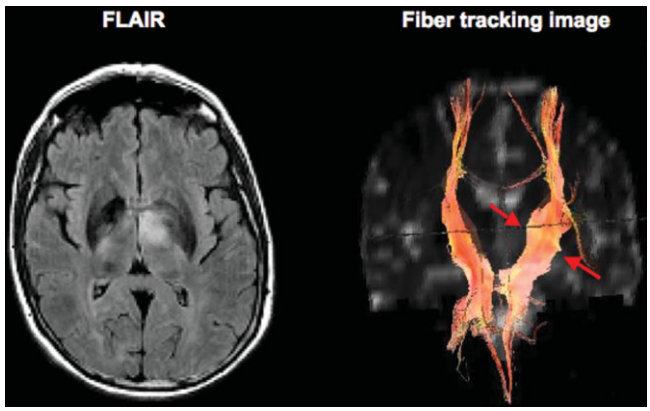

Figure 6. Using diffusion effects to generate maps of white matter tracts. Axial FLAIR image shows a low-grade glioma. Tractography map generated from diffusion tensor source images shows expansion of the corticospinal tract running through the tumor (arrows) compared to the normal compact tract on the opposite side. This method may become useful as a preoperative tool to determine the relationship between tumors and important white matter tracts.

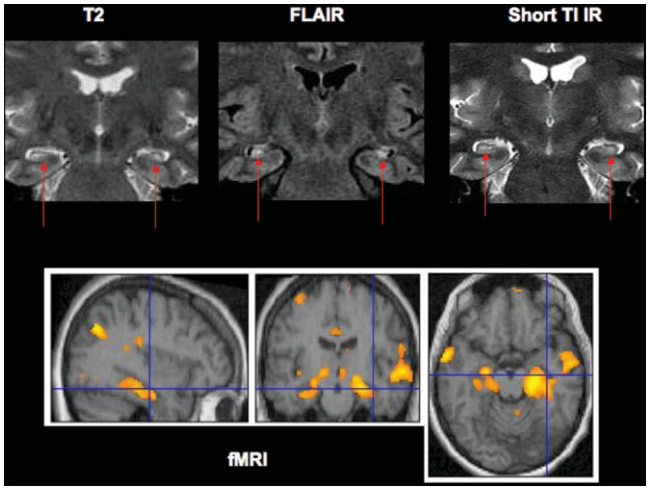

Figure 7. Epilepsy protocol. Top row of images show the coronal sequences applied for assessment of patients with temporal lobe epilepsy. The FLAIR and T2 images are obtained to determine if gliosis, which typically produces increased T2 signal, is present. The short TI IR image with long TE provides more detailed anatomy for determining the presence of hippocampal atrophy. Together, the findings of gliosis and atrophy indicate the presence of mesial temporal sclerosis. Arrows point to the hippocampus, showing bilateral mesial temporal sclerosis in this patient. The bottom row of images is from an fMRI experiment performed to assess working memory in a different patient with temporal lobe epilepsy. Considerable bilateral hippocampal activation during this memory task is present.

between the vascular and stationary protons. The second method does not depend on saturation or inflow to produce this contrast, but on increased T1 relaxation of blood signal produced by a bolus of intravenous Gd. The latter technique is constrained by the need to image a Gd bolus passing through the vessels of interest. The sequence must be fast but with high spatial resolution. This is achieved by using a fast 3D gradient echo sequence with centric ordering of *k*-space (18). A coronal acquisition can yield high quality cervicocerebral vascular anatomy from the aortic arch (Arch) to the circle of Willis (COW) if a neurovascular head coil with full head and neck coverage is available (Fig. 9). A higher resolution version can be used for detailed imaging of the intracranial vasculature. These sequences are effective for assessing atheromatous disease, vascular dissections, cerebral aneurysms, etc., with the added benefit of reduced sensitivity to magnetic susceptibility effects caused by vascular appliances (echo times $\approx$ 1 msec with these sequences). The ability to "see through" metal clip and coil artifacts for assessing efficacy of aneurysm occlusion has reduced the need for invasive conventional angiography surveillance in these patients (Fig. 10) (19). If the scan is triggered at the time of maximal venous contrast concentration following passage of the Gd bolus through the arterial circulation, then highly detailed MR venograms can be obtained (Fig. 11).

ISCHEMIC STROKE IMAGING PROTOCOL

The majority of ischemic strokes are caused by clots that occlude cervical or cerebral arteries. Rapid restoration of blood flow through clot dissolution (thrombolysis) is therefore the primary treatment goal. This has been made possible by administration of tissue thromboplastin activator (tPA), an endogenous thrombolytic agent that is administered at high concentration. Although effective, tPA carries with it the risk of producing hemorrhage within the ischemic tissue, thus increasing morbidity and mortality. In fact, the rate of hemorrhagic transformation (HT) may increase by 10-fold when tPA is used (20). This study indicated that the risk was unacceptably high unless tPA was restricted to within three hours of symptoms for intravenous administration. The PROACT study (21) defined a six-hour guideline for intraarterial administration. These issues impose important requirements on the imaging workup of these patients, including the need for functional/physiological information. Both computed tomography (CT) and MRI have been advocated, and there are compelling reasons for each, with strong advocates in both camps (it is beyond the scope of this review to address this debate in detail).

Regardless of imaging modality, fundamental principles apply. These include:

- Diagnosis
- Detection of hemorrhage
- Arch to COW angiography
- Penumbra imaging
- Speed

The first goal is to establish the diagnosis of arterial ischemic stroke (AIS) and exclude other causes of acute neurological deficit such as primary brain hemorrhage. It is also necessary to look for evidence of bleeding into the infarct since this would be a contraindication to thrombolysis. The presence and location of thrombus in the arterial tree must be determined, especially if

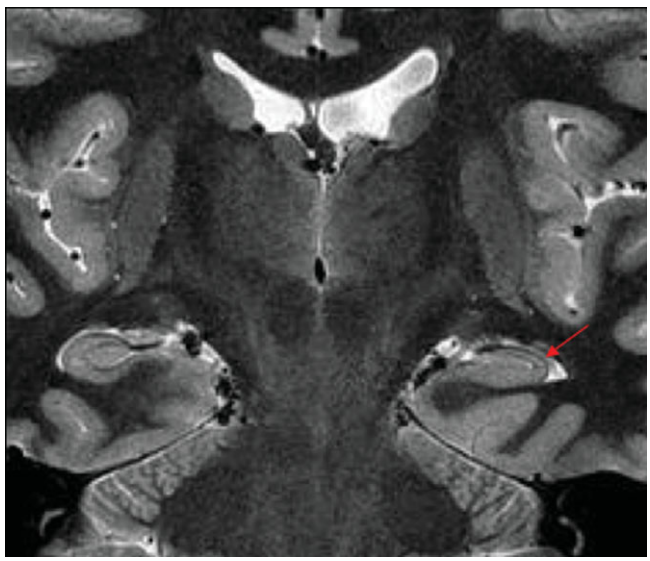

Figure 8. High-resolution anatomical imaging using IR prepped T2 imaging. Short TI IR image with long TR and TE performed at 3T showing improvement in the anatomical rendition of the hippocampus in a patient with left temporal lobe epilepsy. The left hippocampus shows atrophy (arrow) correlating with the reported EEG abnormalities.

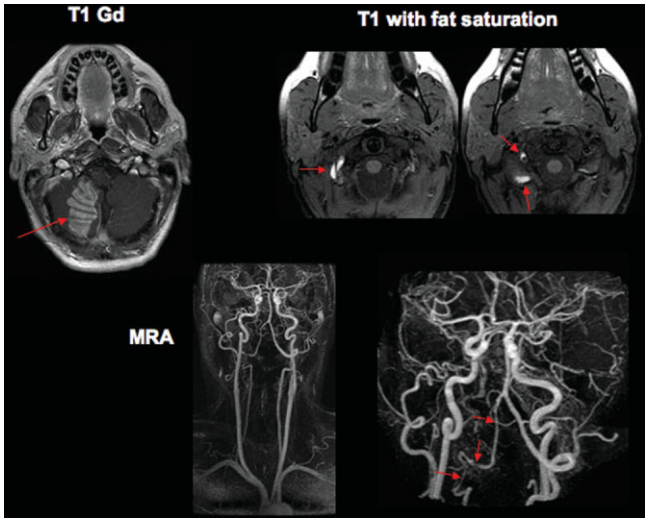

Figure 9. Effective use of T1 "paint" from the palette for vascular imaging. ATECO MRA shows detailed anatomy of the cervicocerebral vasculature obtained in 2.5 minutes of imaging time including information from the aortic arch to the circle of Willis. Arrows on the lower right image point to narrowing of the lumen of the right vertebral artery (a location where dissections (tears) in the vessel wall) commonly occur. Confirmation is obtained by adding T1 sequences with fat saturation where arrows point to blood in the form of methemoglobin (paramagnetic and therefore bright on T1 image) present in the wall of the vertebral artery. The arrow in the T1-Gd image shows enhancement typical of a cerebellar infarct caused by occlusion of a branch of the right vertebral artery (the posterior inferior cerebellar artery).

intraarterial thrombolysis is being considered. The role of penumbra imaging continues to be controversial, but most consider evidence of penumbra necessary for initiation or continuation of thrombolytic therapy. Penumbra refers to that tissue which can be rescued if perfusion is reestablished. It represents underperfused but viable tissue surrounding the core of the infarct. Finally, time is of the essence. It has been reported that 1.9 million neurons per minute are irreversibly lost in the initial phases of AIS (22). Protocols should therefore be as short as possible without compromising the information needed for patient management. How can this be achieved? No universally accepted MRI protocol exists for AIS imaging. We have implemented a protocol at our institution that follows the previously described guidelines. The key to the protocol has been to utilize the time efficiency of EPI with the functional information available with EPI to generate an EPI dominated protocol. We have chosen from the imaging palette sequences that depend primarily on T1, diffusion-weighted imaging (DWI), and T2* relaxation to fulfill these needs (Fig. 12). The protocol is as follows:

1. Localizer (multiplanar): 11 seconds
2. Axial T1 FSE: 42 seconds
3. Axial EPI-diffusion: 40 seconds
4. Axial EPI-FLAIR: 40 seconds
5. Axial EPI-gradient echo (iron sequence): 18 seconds
6. Axial EPI-gradient echo (perfusion): 45 seconds
7. Coronal autotriggering and elliptic centric ordering (ATECO) MRA (Arch to COW): 150 seconds
8. Axial T1 FSE: 116 seconds

The axial T1 sequence is an anatomical sequence that is also useful to exclude the presence of laminar necrosis (band of increased signal within the gray matter) in order to screen for previous subacute or chronic infarction. The diffusion sequence, from which a calculated ADC image is obtained, is used to identify acutely infarcted tissue that characteristically shows reduced or restricted water diffusion. The EPI FLAIR sequence is used to rapidly screen for brain lesions that have a long T2 relaxation. The EPI gradient echo sequence is sensitive to all types of hemorrhage from hyperacute through chronic stages. Next, a perfusion sequence is obtained, requiring a rapidly administered bolus of Gd (5 cc/second for a total of 15 cc). producing a transient signal loss due to T2* effects as the bolus passes through the microcirculation, thus enabling calculation of perfusion images. The diffusion images are then compared with the perfusion images to determine if salvageable tissue is present. Penumbra is identified as that tissue outside the zone of restricted diffusion that shows reduced perfusion on a calculated image, which is usually based on mean transit time. A second Gd bolus is then administered with a 3D gradient echo in the coronal plane using ATECO of *k*-space (18). This sequence is fast and provides detailed information about the vasculature from the aortic arch through the COW. It is also insensitive to previous administration of

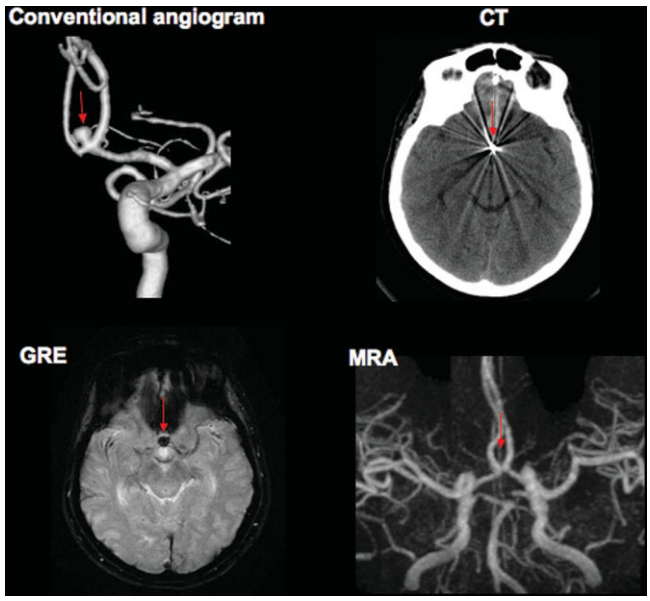

Figure 10. Contrast-enhanced MRA. The conventional angiogram shows an anterior communicating artery aneurysm (arrow) that was treated via deposition of platinum coils using catheter techniques. Noninvasive follow-up imaging presents a problem for CT and MR due to coil artifacts (see arrows on CT and gradient recalled echo [GRE] sequence). ATECO MRA solves the problem, as the exceptionally short TEs employed sharply reduce signal loss caused by magnetic susceptibility effects arising from the coils. The MRA used to follow this patient shows that the aneurysm remains fully occluded.

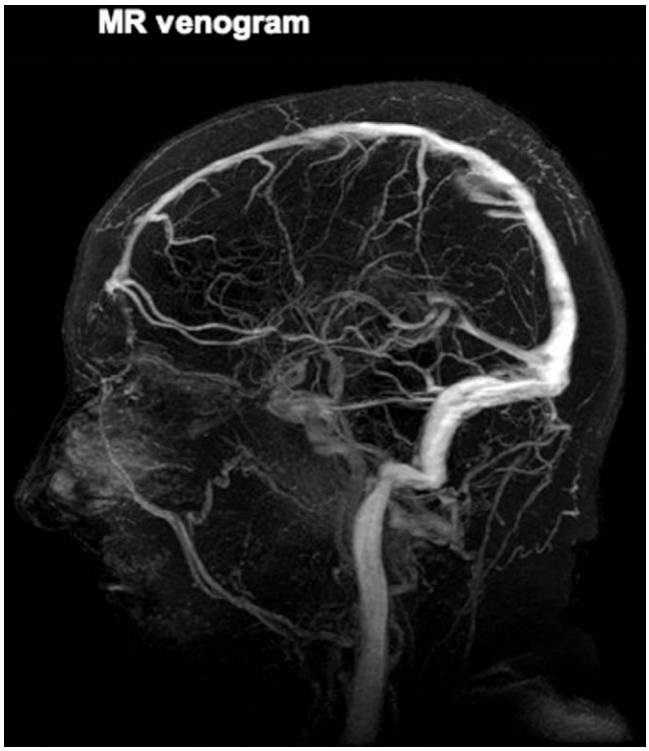

Figure 11. Contrast-enhanced MRA. ATECO MR venography (MRV) acquisitions are obtained by delayed triggering of the sequence, to capture maximal venous filling during passage of the rapidly injected Gd.

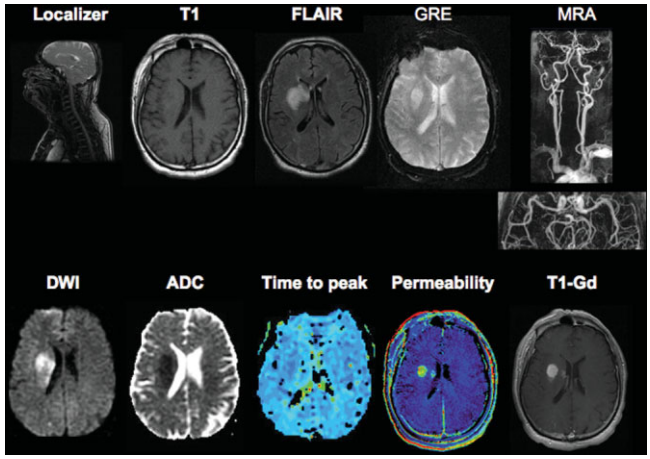

Figure 12. Acute stroke protocol. This patient was studied 18 hours after onset of symptoms (not a tPA candidate). No abnormality is visible on T1 but the FLAIR image shows edema in this late acute infarct. There is no hemorrhage based on the gradient recalled echo [GRE]. MRA shows fully patent vessels. DWI and the associated ADC map indicate the extent of the infarcted tissue. The perfusion map, which displays the arrival time of the Gd bolus, shows no abnormality, which is in keeping with open vessels. The permeability map shows considerable leak in the blood brain barrier, which was confirmed on the T1-Gd image. A small hemorrhage developed in the area of the permeability defect on the 48-hour follow-up (not shown).

Gd (personal experience). The final axial T1 sequence is obtained to look for evidence of contrast enhancement within the infarct. It has been shown that Gd enhancement in a hyperacute infarct is positively correlated with HT of the infarct (23). As an outgrowth of this we are now actively assessing the integrity of the BBB using a third bolus (given as the next sequence after number five above) to assess the magnitude of the permeability defect since there is evidence of a correlation between the degree of permeability increase and HT (24). It may be possible to quantify the risk of HT at the time of presentation. This information might prove especially useful in patients in whom the onset of stroke is unknown and who are therefore excluded from potentially beneficial tPA treatment.

SPINE IMAGING PROTOCOL

Spinal imaging presents a more significant anatomical challenge than brain imaging. The spine is a long curving target containing the spinal cord, which is completely surrounded by a magnetically inhospitable bony vertebral column. Linear arrays of "receive only" surface coils are needed to enable both large and small FOVs to screen multiple segments and to more closely examine individual segments in detail. Body coil radio frequency (RF) transmission is required, with the drawback of increasing energy deposition into the tissues. Although the spinal cord is an integral part of the CNS and suffers from many of the same diseases, functional imaging tools commonly applied to brain imaging, such as fMRI, DTI, and MRS, are very difficult to implement due to the magnetic field distortions caused by the vertebral column. Spinal imaging becomes an even greater challenge at filed strengths above 1.5T due to greater RF demands (increased specific absorption rate [SAR]) and increased bone-related susceptibility effects. Fortunately, the majority of spinal imaging is performed to assess the clinical consequences of degenerative disc disease and conventional T1, T2, and gradient echo

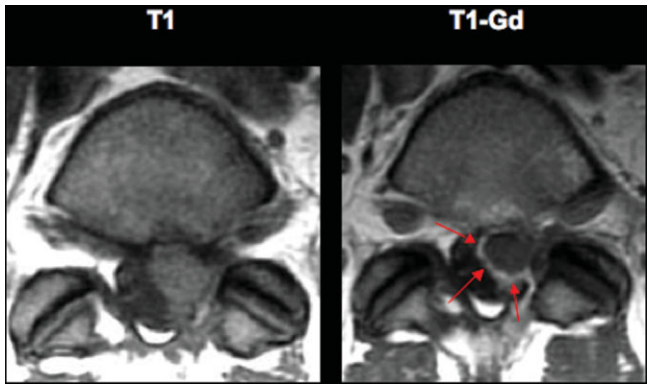

Figure 13. Utility of T1-Gd imaging in the postoperative spine. This patient was referred for assessment of recurrence of symptoms one year following disc removal. The most common causes for "failed back syndrome" are scar tissue vs. disc herniation. The T1 image shows soft tissue in the epidural space. Scar tissue will enhance almost indefinitely after surgery. Disc material, which is avascular, does not typically enhance. The T1-Gd image shows edge enhancement from a small amount of scar (arrows) surrounding a large recurrent nonenhancing disc herniation.

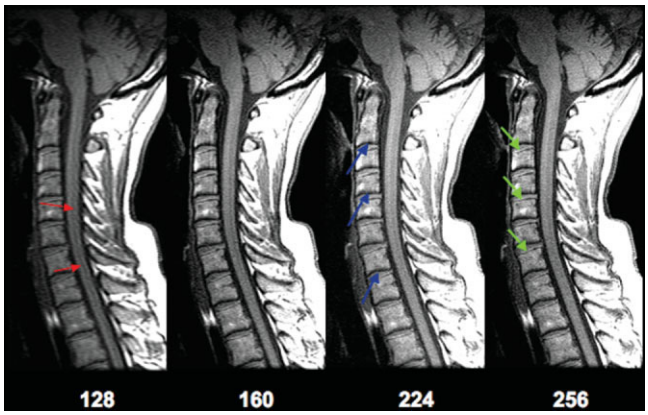

Figure 14. Gibbs artifact. T1 images with increasing phase encoding from 128 to 256 show reduction of the dark curvilinear signal in the spinal cord (red arrows) representing Gibbs artifact. This can be confused with the presence of a syrinx cavity since it can also appear as a bright line on T2 images. Chemical shift artifact is visible along the inferior surface of each vertebral body (blue arrows) due to displacement of the marrow fat superiorly (the frequency encoding direction). The superior endplates (yellow arrows) are seen less well due to the high signal from the displaced fat.

imaging sequences are applicable. Sagittal T1 and T2 sequences provide an excellent screen for all types of spinal cord, bone, and disc pathology, and are the foundation for all spinal MRI. Sequence modifications that eliminate fat signal either using short TI IR or frequency-selective fat saturation, are very useful for assessing the presence of diseases infiltrating bone marrow (metastases) or for assessing posttraumatic soft tissue injury. When applying axial sequences for evaluating individual segments or discs, the acquisitions must be adjusted to properly examine the exiting foramina (neural foramina) of the spinal nerve roots. This is especially challenging in the cervical spine, where the neural foramina are less than 1 cm in size, compared to 2 cm in the lumbar spine. It has been our philosophy to limit axial slice thicknesses in the cervical spine to a maximum of 2.5 mm in order to more accurately gauge the narrowing effect of herniated discs and osteophytes (bone spurs) arising for the uncovertebral and facet joints. This can be achieved with 3D methods, usually consisting of T2-weighted gradient echo or spin-echo techniques. T2 weighting results in high CSF signal juxtaposed to the lower signal of herniated discs, osteophytes, and spinal cord, enabling accurate assessment of the compressive effect of degenerating discs on the neural elements. Axial T2 sequences are also used for thoracic and lumbar imaging, although 2D methods are more commonly applied since coverage can be extended for screening the longer spinal segments. The most common application of Gd in spinal imaging is for assessing the presence of recurrent disc herniation vs. postoperative scar tissue (Fig. 13). It is also applied for any condition in which disruption of the blood brain (spine) barrier is suspected, and can be exceptionally useful when used as a bolus in 3D MRA methods for defining the presence of abnormal vessels in the subarachnoid space secondary to the presence of arteriovenous malformations (AVMs). Not only can the presence of AVMs be confirmed, but the level of the feeding artery can be ascertained with high confidence (18). This has had a major impact on planning and guiding conventional and therapeutic angiography.

ARTIFACTS AND PITFALLS

Image artifacts can be divided into three broad categories: 1) those that are caused by faulty elements in components of the MR system and site; 2) those that are the result of imperfections in the imaging sequences and their anatomical targets; and 3) those that are produced by the anatomy and physiology of the target. Since this is a large topic beyond the scope of this work (25), only the more commonly encountered artifacts will be discussed. Common category one artifacts are streaking and banding. The streaking artifact has the appearance of thin line, a few pixels wide, with random intensity projected along the phase encoding direction. It is caused by extraneous RF brought into the scanner room by an electronic device, defect in the RF shield, or incomplete closure of the scanner room door. The band or stripe artifact is seen as parallel bands of decreased signal spread across the image caused by a single corrupt point in *k*-space. The frequency and orientation of the bands are dependent on the location of the point in

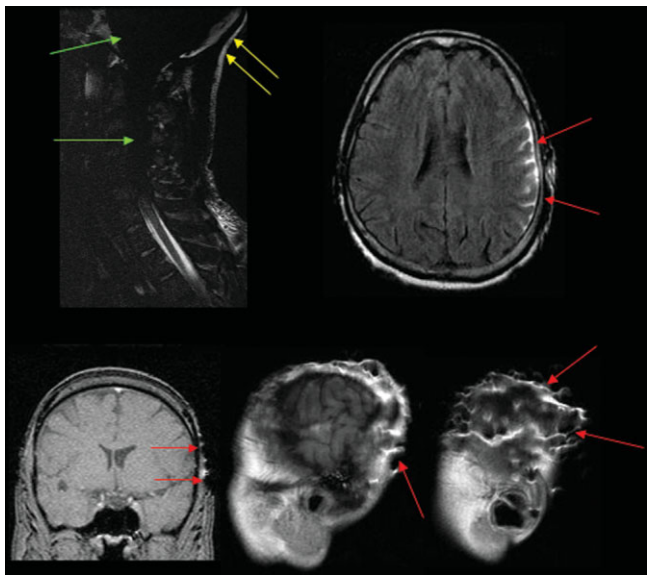

Figure 15. Off-resonance artifacts. The upper left image is a sagittal T2 image of the cervical spine acquired with fat saturation. Magnetic field inhomogeneities shift the water resonance into the fat frequency. Signal from water protons in the brain, spinal cord, and CSF are thereby extinguished (green arrows). Note that the fat protons in the scalp fat are preserved (yellow arrows). Off-resonance artifacts can also lead to signal increases. When FLAIR sequences are applied in regions of field inhomogeneity (caused in this example by surgical scalp clips—red arrows on lower images), the off-resonance water protons in the vicinity of the clips are only partially inverted by the 180° inversion pulse. The subsequent 90° RF pulse finds nonzero magnetization producing high signal in the CSF (red arrows upper left image). This can easily be misinterpreted as subarachnoid hemorrhage.

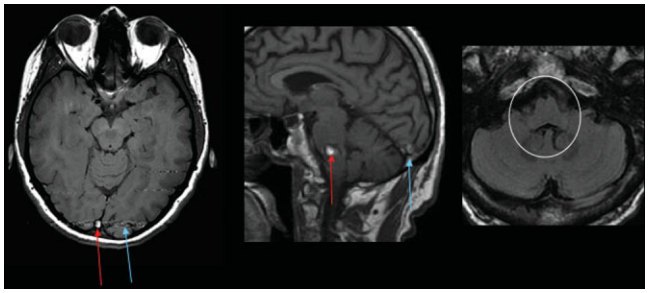

Figure 16. Phase artifacts. Pulsating blood in the superior sagittal sinus (red arrow on left image) is responsible for the phase artifact displayed across the image on a line (blue arrow). This artifact will not be confused with a lesion, but the phase artifact in the middle image (red arrow), also produced by the superior sagittal sinus (blue arrow), is more coherent and can easily be misinterpreted as a hemorrhagic lesion. Cross-correlation with the axial image on the right shows no lesion proving the presence of an artifact.

k-space. Common category 2 artifacts include truncation, chemical shift, and unintentional water saturation. Truncation, also called Gibbs artifact, is a ringing artifact of the Fourier transform producing alternating bands in the proximity of a sharp interface between high and low signal. They can occur in either the phase or readout directions and are minimized by increasing the spatial resolution in the direction of the artifact (Fig. 14). There are variety of chemical shift artifacts that occur as a result of the 3.5 ppm difference in resonant frequency between water and fat. Since proton location in an image is based on a smooth linear change in precessional frequencies during application of readout gradient, fat protons resonating at a different frequency from water protons are displaced away from their true positions in the frequency encode direction. This effect can be seen in almost every sagittal T1 sequence of the spine (Fig. 14). Other chemical shift related artifacts, perhaps more accurately termed "off resonance" effects, are the inadvertent saturation of water protons when frequency-selective fat saturation is applied. If the resonant frequency of water protons in some part of the FOV is shifted into the fat frequency, then the water signal will be lost (Fig. 15). This is usually caused by regional magnetic field inhomogeneities in tissues. Shimming can help to alleviate the artifacts. Another example of this is the shift in resonant frequency of nearby water protons caused by local metallic implants. In this case, increased as opposed to absent water signal was seen in the vicinity of the clips on FLAIR sequences due to incomplete inversion of the off-resonance water protons by the 180° inversion pulse (Fig. 15). The most common example of category 3 artifact is phase artifact produced by movement of protons during application of the phase encoding gradient. It is seen as a repeating image of the structure displaced on a line including the original structure in the phase encoding direction. Occasionally, these artifacts can produce "pseudolesions" (see Fig. 16). The key to avoiding misinterpretation is to try to identify the abnormality on another sequence and in another imaging plane. If the abnormality persists, it is likely real.

SUMMARY

The protocols discussed here illustrate general principles that are universally applicable. Each user, however, has specific needs, preferences, and categories of patient pathology, and may be constrained by available hardware and software. Each imaging protocol should be the right mix of speed, resolution, and image quality, but because of user specific variables, it is difficult to recommend a standard set of protocols. A solution that has worked effectively at our institution is the establishment of a monthly protocol meeting composed of radiology staff, including MRI technologists, vendor representatives, and MR physicists. Modified and new protocols are reviewed, discussed, and implemented. This forum has been very effective for standardizing protocols across the institution, and for keeping pace with hardware and software changes, thus maximizing the return on capital invested in these imaging systems.

REFERENCES

1. Piguet O, Ridley LJ, Grayson DA, et al. Comparing white matter lesions on T_2 and FLAIR MRI in the Sydney Older Persons Study. Eur J Neurol 2005;12:399–402.
2. Bakshi R, Ariyaratana S, Benedict RH, Jacobs L. Fluid-attenuated inversion recovery magnetic resonance imaging detects cortical and juxtacortical multiple sclerosis lesions. Arch Neurol 2001;58:742–748.
3. Grossman RI, McGowan JC. Perspectives on multiple sclerosis. Am J Neuroradiol 1998;19:1251–1265.
4. Filippi M, Horsfield MA, Hajnal JV, et al. Quantitative assessment of magnetic resonance imaging lesion load in multiple sclerosis. J Neurol Neurosurg Psychiatry 1998;64(Suppl 1):S88–S93.
5. Simon JH, Li D, Traboulsee A, et al. Standardized MR imaging protocol for multiple sclerosis: Consortium of MS Centers consensus guidelines. Am J Neuroradiol 2006;27:455–461.
6. Knopp EA, Cha S, Johnson G, et al. Glial neoplasms: dynamic contrast-enhanced T2*-weighted MR imaging. Radiology 1999;211:791–798.
7. Patankar TF, Haroon HA, Mills SJ, et al. Is volume transfer coefficient (K(trans)) related to histologic grade in human gliomas? Am J Neuroradiol 2005;26:2455–2465.
8. Roberts HC, Roberts TP, Brasch RC, Dillon WP. Quantitative measurement of microvascular permeability in human brain tumors achieved using dynamic contrast-enhanced MR imaging: correlation with histologic grade. Am J Neuroradiol 2000;21:891–899.
9. Kitis O, Altay H, Calli C, Yunten N, Akalin T, Yurtseven T. Minimum apparent diffusion coefficients in the evaluation of brain tumors. Eur J Radiol 2005;55:393–400.
10. Yamasaki F, Kurisu K, Satoh K, et al. Apparent diffusion coefficient of human brain tumors at MR imaging. Radiology 2005;235:985–991.
11. Calvar JA, Meli FJ, Romero C, et al. Characterization of brain tumors by MRS, DWI and Ki-67 labeling index. J Neurooncol 2005;72:273–280.
12. Roessler K, Donat M, Lanzenberger R, et al. Evaluation of preoperative high magnetic field motor functional MRI (3 Tesla) in glioma patients by navigated electrocortical stimulation and postoperative outcome. J Neurol Neurosurg Psychiatry 2005;76:1152–1157.
13. Keles GE, Berger MS. Advances in neurosurgical technique in the current management of brain tumors. Semin Oncol 2004;31:659–665.

14. Berman JI, Berger MS, Mukherjee P, Henry RG. Diffusion-tensor imaging-guided tracking of fibers of the pyramidal tract combined with intraoperative cortical stimulation mapping in patients with gliomas. J Neurosurg 2004;101:66–72.
15. Bartolomei F, Khalil M, Wendling F, et al. Entorhinal cortex involvement in human mesial temporal lobe epilepsy: an electrophysiologic and volumetric study. Epilepsia 2005;46:677–687.
16. Wu WC, Huang CC, Chung HW, et al. Hippocampal alterations in children with temporal lobe epilepsy with or without a history of febrile convulsions: evaluations with MR volumetry and proton MR spectroscopy. Am J Neuroradiol 2005;26:1270–1275.
17. Varho T, Komu M, Sonninen P, Lahdetie J, Holopainen IE. Quantitative HMRS and MRI volumetry indicate neuronal damage in the hippocampus of children with focal epilepsy and infrequent seizures. Epilepsia 2005;46:696–703.
18. Farb RI, McGregor C, Kim JK, et al. Intracranial arteriovenous malformations: real-time auto-triggered elliptic centric-ordered 3D gadolinium-enhanced MR angiography—initial assessment. Radiology 2001;220:244–251.
19. Farb RI, Nag S, Scott JN, et al. Surveillance of intracranial aneurysms treated with detachable coils: a comparison of MRA techniques. Neuroradiology 2005;47:507–515.
20. The NINDS t-PA Stroke Study Group. Intracerebral hemorrhage after intravenous t-PA therapy for ischemic stroke. Stroke 1997; 28:2109–2118.
21. Furlan A, Higashida R, Wechsler L, et al. Intra-arterial prourokinase for acute ischemic stroke: the PROACT II Study: a randomized clinical trial. JAMA 1999;282:2003–2011.
22. Saver JL. Time is brain—quantified. Stroke 2006;37:263–266.
23. Kim EY, Na DG, Kim SS, Lee KH, Ryoo JW, Kim HK. Prediction of hemorrhagic transformation in acute ischemic stroke: role of diffusion-weighted imaging and early parenchymal enhancement. Am J Neuroradiol 2005;26:1050–1055.
24. Kassner A, Roberts T, Taylor K, Silver F, Mikulis D. Prediction of hemorrhage in acute ischemic stroke using permeability MR imaging. Am J Neuroradiol 2005;26:2213–2217.
25. Zhuo T, Gullapalli RP. MR artifacts, safety, and quality control. Radiographics 2006;26:275–220.